ELSEVIER

Biochimica et Biophysica Acta 1420 (1999) 266–271

BIOCHIMICA ET BIOPHYSICA ACTA
BBA

www.elsevier.com/locate/bba

Rapid report

Lag-burst kinetics in phospholipase A_2 hydrolysis of DPPC bilayers visualized by atomic force microscopy

Lars K. Nielsen [a,b], Jens Risbo [b], Thomas H. Callisen [a,1], Thomas Bjørnholm [b,*]

[a] *Department of Chemistry, Technical University of Denmark, DK-2800 Lyngby, Denmark*

[b] *CISMI, Laboratories of Materials Science, Department of Chemistry, University of Copenhagen, Fruebjergvej 3, DK-2100 Copenhagen Ø, Denmark*

Received 8 June 1999; accepted 17 June 1999

Abstract

The lag-burst phenomenon in the phospholipase A_2 mediated hydrolysis of phospholipid bilayers is for the first time demonstrated in an atomic force microscopy (AFM) study. Simultaneous AFM measurements of the degree of bilayer degradation and the physical-chemical state of the membrane reveals growing nanoscale indentations in the membrane during the lag phase. It is argued that these indentations are domains of hydrolysis products (lysoPC/PC) which eventually trigger the burst. The rate of the rapid hydrolysis following the burst is found to be proportional to the length of the edge between membrane adsorbed and desorbed to the mica base. The observed maximal rate of membrane degradation is approx. 0.2 mmol lipid/min/mol lipase in solution.

Keywords: Lag burst; Atomic force microscopy; Phospholipase A_2; Supported bilayer; Enzyme kinetics; Nano chemistry

Phospholipase A_2 (PLA_2) is a water-soluble enzyme which catalyzes the regio-specific hydrolysis of the *sn*-2 acyl ester linkage of *sn*-glycero-3-phospholipids. The products are fatty acids (FA) and 1-acyl-lysophospholipids (lysoPC) [1]. The understanding of this thoroughly studied reaction is important to many physiological processes such as lipid metabolism, immunological response, and digestive reactions [2]. PLA_2 is an interfacially activated enzyme [1,3–5] and its activity as well as the hydrolysis kinetics depend on the morphology and the physico-chemical state of the substrate [6].

The kinetics of the PLA_2 hydrolysis of bilayer substrates under certain conditions exhibit so-called lag-burst behavior, where the rate of hydrolysis suddenly changes from a regime of low activity to a regime of rapid hydrolysis [7–9]. The duration of the slow hydrolysis regime or lag phase, the lag time, depends on a number of properties of the system including substrate concentration, calcium concentration, and accumulation of products in the bilayer. The degree of compositional heterogeneity and the number of bilayer defects have for example been correlated to the duration of the lag time; a large number of defects leads to no or short lag time and vice versa [10,11].

Despite the intense investigations of the lag-burst kinetics the underlying mechanism of the phenomenon is still poorly understood. In the light of this the strategy of the present study has been to repeat some

* Corresponding author. E-mail: tb@symbion.ki.ku.dk

[1] Present address: Novo Nordisk A/S, Novo Allé, DK-2880 Bagsværd, Denmark.

0005-2736/99/$ – see front matter
PII: S0005-2736(99)00103-0

of the above mentioned experiments [10,11] in the liquid cell of an atomic force microscope (AFM) in order to allow direct comparisons to previous results. In addition to this we also gain new insight into the changes occurring in the bilayer at the nanometer scale also during the lag period.

The use of AFM to image biological material in its native environment is well established [12]. Scanning under buffer has for example allowed real-time imaging of biological processes such as enzymatic action with extremely high lateral resolution. Measurements on single enzyme molecules have recently been performed [13]. Supported lipid bilayers, used as substrate for PLA_2, have proven to be very suitable for non-destructive AFM imaging [12,14].

In the present study snake venom PLA_2 from *Agkistrodon piscivorus piscivorus* (Sigma, St. Louis, MO) was purified according to Maraganore et al. [16]. PLA_2 concentration was determined by absorbance at 280 nm using an extinction coefficient of 2.2 ml/mg/cm. Dipalmitoylphosphatidylcholine (DPPC; Avanti Polar Lipids, Alabaster, AL) was used without further purification. A HEPES buffer (10 mM HEPES (pH 8.0), 150 mM KCl, 30 μM $CaCl_2$, and 10 μM EDTA) which prevents extensive calcium-palmitate precipitation [17], and minimizes concentration changes of the co-factor Ca^{2+} at the bilayer surface upon formation of negatively charged fatty acids [18] was used. The enzyme with these buffer conditions is known to show lag-burst kinetics with vesicular substrates [10,11].

Supported DPPC bilayers were prepared on a commercial Langmuir trough (KSV 5000, KSV, Finland) using freshly cleaved mica as solid support. DPPC was dissolved in *n*-hexane (HPLC grade) to a concentration of 0.6 mg/ml and spread on pure Milli-Q water surface. Solvent evaporation was allowed for 30 min prior to monolayer compression at a constant velocity of 1 $Å^2$/molecule/min to a final surface pressure of 30 mN/m. Two layers were then transferred vertically at 20°C at a constant speed of 1 mm/min, waiting 15 min between the first and second layer. The supported bilayers were subsequently transferred to the fluid cell of the AFM (Nanoscope IIIa, Digital Instruments, Santa Barbara, CA). A standard silicon O-ring was used to seal the fluid cell. HEPES buffer without enzyme was used to flush the fluid cell prior to the actual imaging. Scanning

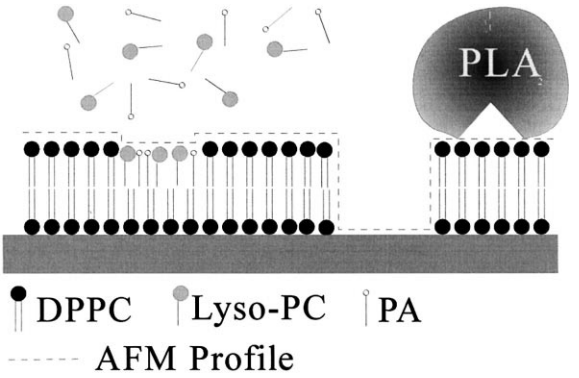

Fig. 1. Schematic illustration of the experimental setup, illustrating how the enzymatic hydrolysis by PLA_2 is recorded by the AFM. The mica supported bilayer is hydrolyzed by PLA_2 and as the products dissolve in the buffer areas with bilayer deep defects are recorded by the AFM tip. Such defects are defined as the primary observable in the experiment and they are used as a measure of the degree of hydrolysis. Regions with an intermediate height comprised of product molecules can also be detected. The broken line indicates the surface topography recorded by the AFM tip.

was carried out using oxide sharpened silicon nitride tips (NanoProbes, Santa Barbara, CA) with a nominal spring constant of 0.06 N/m. The bilayer was equilibrated for 30 min before injection of the same buffer containing 84 nM PLA_2. Imaging was carried out in contact mode with a loading force of less than 500 pN at room temperature (25°C). Fig. 1 shows a schematic illustration of the process of PLA_2 hydrolysis of a supported DPPC bilayer and the data acquired by the AFM. The supported bilayer is hydrolyzed by PLA_2 and as the products dissolve in the buffer areas with bilayer deep defects occur. These defects are our primary observable. Quantitative data for the enzyme kinetics are obtained by equating the degree of hydrolysis to the total area of the bilayer deep defects.

Image analysis was carried out on a Macintosh computer using the public domain program Image SXM (available on the internet http://rsb.info.nih.gov/nih-image). A binarization of the images is performed which readily allows the degree of membrane desorption to be determined. In the present study we define the relative amount of desorbed membrane as the ratio between the area covered with a bilayer thick membrane (incl. possible product domains) and the area of visible mica (Fig. 2). The length of

the edge around the intact bilayer has also been determined using Image SXM.

A time sequence of AFM images from an experiment on a bilayer transferred in the gel phase (30 mN/m) is shown in Fig. 2. Fig. 2A shows the initial bilayer which is devoid of any large defects within the frame of view. After the enzyme is injected the bilayer is hydrolyzed by PLA_2 and large defect areas develop where the bilayer has been hydrolyzed and the products dissolved (dark areas in Fig. 2B–D). The low calcium concentration in the buffer and the overall lipid concentration of around 2 μM (just below the CMC of the products) make the products soluble in the buffer. The affinity of the products for the bilayer may prevent solubilization until a certain domain size has been reached. In addition, product areas are known to be unstable under mechanical stress [19]. The mechanical influence of the tip, although minimized, may thus contribute to product dissolution. The generated defects allow

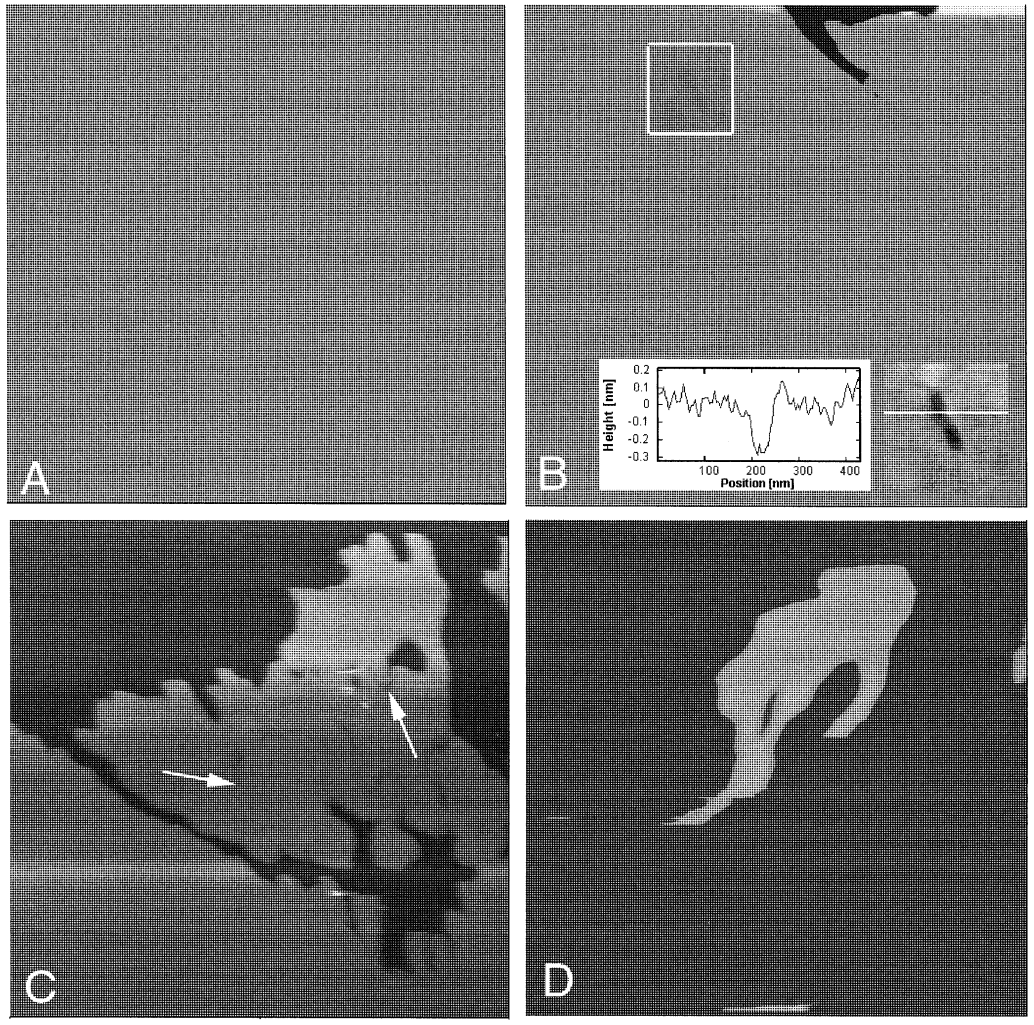

Fig. 2. AFM images of a time sequence of the PLA_2 hydrolysis of supported DPPC bilayer on mica transferred at 30 mN/m. (A) Image prior to PLA_2 injection, and (B) 8 min, (C) 14 min, (D) 17 min, respectively, after PLA_2 injection. Light gray areas correspond to intact bilayer whereas dark areas correspond to the mica support. In B the inserts show a software zoom of the boxed area with one of several small depressions observed with a typical depth of 0.4–0.7 nm (gray scale has been extended to clearly show the depression); also shown is a section through the zoomed image. Arrows in C indicate small narrow channels, 15–20 nm wide, which are presumably created by a single enzyme molecule. Image size 2×2 μm. Gray scale 10 nm. Images have been corrected for baseline tilt and bow.

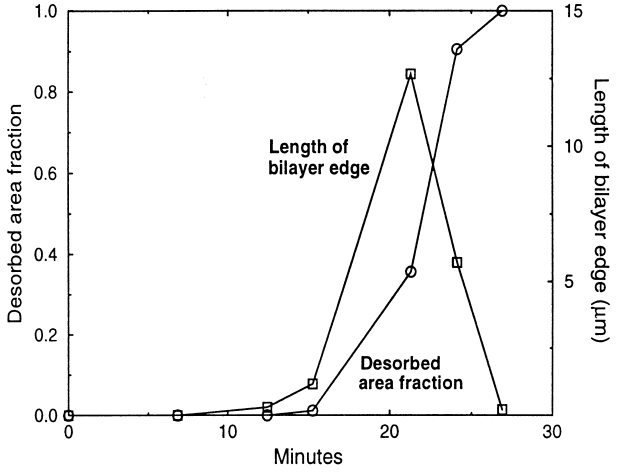

Fig. 3. Analysis of the complete image series of Fig. 2 (including frames not shown in the figure). The graph shows the hydrolyzed area fraction and the length of the bilayer edge as functions of time. The lag-burst kinetics is clearly illustrated as the sudden change between 8 and 14 min. The lag time is estimated to be 8–10 min.

measurement of the thickness of the bilayer which is found to be close to 6 nm in agreement with previous data [12,20]. As a control a large area was scanned to confirm that hydrolysis has taken place over the entire sample. Since there is no visible difference between the degradation of the areas that have been continuously scanned and those which have not, we may exclude that the observed hydrolysis is influenced by the scanning probe.

In the lag phase, which for the experiment shown in Fig. 2 is the first 8–10 min after enzyme injection, small but significant changes in the bilayer occurs. The changes in the lag phase are illustrated in Fig. 2B where the insert shows how small depressions evolve. These depressions, of 0.3–0.5 nm in depth, are interpreted as areas where the beginning enzyme hydrolysis has caused an increase in product concentration. The domains formed in the bilayer during the lag phase are always observed very close to the burst and thus seem to play an important role in the triggering of the burst.

Image analysis of the complete sequence (eight images) illustrates the enzyme kinetics observed in the experiment as shown in Fig. 3. Lag-burst kinetics is clearly demonstrated by the analysis as a sudden increase in the degree of hydrolysis between 8 and 14 min. The lag time is estimated to be 8–10 min which is comparable to the lag time observed for vesicular substrates [10]. In a number of similar experiments the lag time is found to vary for different experiments depending on preparation procedures (substrates prepared form double layers or vesicles for example) as discussed in a forthcoming paper [23].

In the regime of high enzyme activity the maximum speed of hydrolysis of the supported bilayer can be estimated. As an upper estimate a maximum hydrolysis rate of 20%/min is taken. This leads to a rate of 0.2 mmol DPPC/min/mol PLA_2 in solution which is roughly a thousand times slower than for rapid hydrolysis of vesicular substrates. The difference may readily be explained by the localization of the substrate in the fluid cell of the AFM allowing only a fraction of the injected lipase to actually bind to the substrate. Observation of lag-burst kinetics with a lipase to lipid ratio of 1:25, compared to 1:1000 for vesicular substrates, further illustrates the effect of the localized bilayer. Such high enzyme to lipid ratios would generally abolish a lag phase.

In all our experiments we find a correlation between the maximum length around the edge of the intact bilayer at any point during the hydrolysis, and the maximum rate of PLA_2 hydrolysis. This is clearly

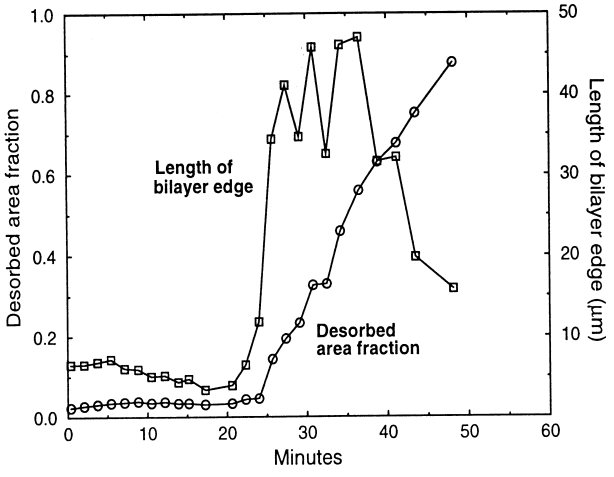

Fig. 4. Analysis of another image series with a larger scan area of 5×5 μm. The lag time of this experiment is somewhat longer than the one presented in Fig. 2. The curves illustrate the correlation between the speed of hydrolysis and the length of the bilayer edge. When the length of the bilayer edge is large the number of potential attack points for the enzyme will also be large thus leading to the maximum hydrolysis speed observed.

observed in Fig. 4 which shows another reaction sequence with more data points. After the burst our observations agree well with the general conception that line defects or other heterogeneity serve as starting points for the enzymatic attack [15,21,22]. Thus when the length of the bilayer edge is large, a large number of potential attack points for the enzyme exist which can be directly correlated to the rate of hydrolysis. A quantitative relation of the derivative of the desorbed bilayer fraction (A) and the length of the bilayer edge (L) can be made. The relation we find from the analysis presented in Fig. 4 is:

$$v = \frac{dA}{dt} \approx 0.022\ \mu m/min \cdot L$$

If the enzymes are only hydrolyzing along the available edge after the burst a new estimate for the hydrolysis speed can be made. For this estimate we assume a mean area per lipid molecule of 45 Å^2 and that the enzymes have a diameter of 5 nm and are closely packed along the edge. With a maximum bilayer edge length of 40 μm the speed of hydrolysis is 250 mol DPPC/min/mol lipase or roughly 10^6 times faster than when the calculation is performed for all the lipase in solution. This number is of course biased by any solubilization of non-hydrolyzed lipid molecules.

Small channels of a width of 15–20 nm are observed during the hydrolysis (Fig. 2B,C) which is a characteristic feature of the hydrolysis of supported bilayers [15]. Such channels have been convincingly argued to be the result of single enzyme molecules hydrolyzing their way through the bilayer [15]. In this case the enzyme turnover has been estimated to be 88 mol DPPC/s/mol for a single enzyme [15].

In summary, the hydrolysis of the supported bilayer follows the following pattern as observed with the AFM. After the injection of the lipase a lag phase is observed with only very few visible changes in the bilayer. Near the burst in activity beginning hydrolysis is observed leading to the formation of small depressions in the bilayer which are interpreted as product enriched domains (see insert of Fig. 2B). Despite the overall low lipid concentration the products initially remain associated with the bilayer. Images of bilayers made of both products and substrate molecules show that areas with the same appearance as the small depressions exist in such mixtures [23]. This strongly supports the interpretation of the small depressions as being product domains generated by the enzyme in the lag phase. The increased bilayer heterogeneity caused by the beginning hydrolysis is assumed to play an important role in the triggering of the burst. The dramatic increase in enzyme activity at the burst leads to large areas devoid of lipids which must have solubilized in the buffer due to the instability of larger product domains.

The authors thank O.G. Mouritsen for stimulating discussions. This work was supported by the Danish Natural Science Research Council, the Danish Technical Research Council and the EU under the Biotechnology program 'Lipid Structure and Lipases'.

References

[1] M. Waite, in: D.E. Vance, J. Vance (Eds.), Biochemistry of Lipids, Lipoproteins and Membranes, Elsevier, Amsterdam, 1991, pp. 269–295.
[2] I. Kudo, M. Murakami, S. Hara, K. Inoue, Biochim. Biophys. Acta 117 (1993) 217–231.
[3] D.L. Scott, S.P. White, Z. Otwinoski, W. Yaun, M.H. Gelb, P.B. Sigler, Science 250 (1990) 1541–1546.
[4] G.L. Nelsestuen, M.B. Martinez, Biochemistry 36 (1997) 9081–9086.
[5] I. Panaiotov, M. Ivanova, R. Verger, Curr. Opin. Colloid Interface Sci. 2 (1997) 517–525.
[6] T. Hønger, K. Jørgensen, D. Stokes, R.L. Biltonen, O.G. Mouritsen, Methods Enzymol. 286 (1997) 168–190.
[7] R. Verger, M.C. E Mieras, G.H. de Haas, J. Biol. Chem. 240 (1973) 4023–4034.
[8] R. Apitz-Castro, M.K. Jain, G.H. De Haas, Biochim. Biophys. Acta 688 (1982) 349–356.
[9] W.R. Burack, R.L. Biltonen, Chem. Phys. Lipids 73 (1994) 209–222.
[10] T. Hønger, K. Jørgensen, R.L. Biltonen, O.G. Mouritsen, Biochemistry 35 (1996) 9003–9006.
[11] T.H. Callisen, Y. Talmon, Biochemistry 37 (1998) 10987–10993.
[12] Z. Shao, J. Yang, Q. Rev. Biophys. 28 (1995) 195–251.
[13] M. Radmacher, M. Fritz, H.G. Hansma, P.K. Hansma, Science 265 (1994) 1577–1579.
[14] M. Radmacher, R.W. Tillmann, M. Fritz, H.E. Gaub, Science 257 (1992) 1900–1905.
[15] M. Grandbois, H. Clausen-Schaumann, H. Gaub, Biophys. J. 74 (1998) 2398–2404.
[16] J.M. Maraganore, G.M. Merutka, W. Cho, W. Welches, F.J. Kèzdy, R.L. Heinrikson, J. Biol. Chem. 259 (1984) 13839–13843.
[17] N. Gheriani-Gruszka, S. Almog, R.L. Biltonen, D. Lichtenberg, J. Biol. Chem. 263 (1988) 11808–11813.

[18] M.S. Fernández, R. Mejia, E. Zavala, F. Pacheco, Biochem. Cell Biol. 69 (1991) 722–727.
[19] H. Speijer, P.L.A. Giesen, R.F.A. Zwaal, C.E. Hack, W.T. Hermens, Biophys. J. 70 (1996) 2239–2247.
[20] G. Cevc, D. Marsh, Phospholipid Bilayers, Wiley, New York, 1987.
[21] D.W. Grainger, A. Reichert, H. Ringsdorf, C. Salesse, FEBS Lett. 252 (1989) 73–82.
[22] M. Grandbois, C. Salesse, J. Dufourcq, Thin Solid Films 284, 285 (1996) 743–747.
[23] L.K. Nielsen, K. Balashev, T. Bjørnholm, manuscript in preparation.